

# Dexmedetomidine alleviates cisplatin-induced acute kidney injury by attenuating endoplasmic reticulum stress-induced apoptosis via the $\alpha_2$ AR/PI3K/AKT pathway

YEJING CHAI<sup>1\*</sup>, KANGSHENG ZHU<sup>2,3\*</sup>, CHAO LI<sup>2</sup>, XIAOFAN WANG<sup>3</sup>,  
JUNMEI SHEN<sup>2</sup>, FANGFANG YONG<sup>2</sup> and HUIQUN JIA<sup>2</sup>

Departments of <sup>1</sup>Medical Periodical Press and <sup>2</sup>Anesthesiology,

The Fourth Hospital of Hebei Medical University, Shijiazhuang, Hebei 050011;

<sup>3</sup>Graduate School of Hebei Medical University, Hebei Medical University, Shijiazhuang, Hebei 050017, P.R. China

Received June 30, 2019; Accepted December 11, 2019

DOI: 10.3892/mmr.2020.10962

**Abstract.** Cisplatin (CP) is an effective antineoplastic agent; however, CP-induced acute kidney injury (AKI) seriously affects the prognosis of patients with cancer. Endoplasmic reticulum (ER) stress (ERS)-induced apoptosis serves a pivotal role in the pathogenesis of CP-induced AKI. Dexmedetomidine (Dex), a potent  $\alpha_2$  adrenergic agonist, has been reported to exert protective effects against AKI. However, the protective effects of Dex against CP-induced AKI and the potential molecular mechanisms remain unknown. In the present study, male Sprague-Dawley rats were divided into four groups (n=10/group), as follows: Control group; CP group, rats received an intraperitoneal (i.p.) injection of 5 mg/kg CP; Dex + CP group, rats received an i.p. injection of 25  $\mu$ g/kg Dex immediately after CP treatment; and Dex + CP + atipamezole (Atip) group, rats received an i.p. injection of 250  $\mu$ g/kg Atip, an  $\alpha_2$  adrenoreceptor ( $\alpha_2$ AR) antagonist, and then received the same treatment as the Dex + CP group. Rats were anesthetized and sacrificed 96 h after CP injection. Subsequently, serum blood urea nitrogen (BUN) and serum creatinine (Scr) were analyzed, and kidney samples were collected for analyses. Pathological changes were examined using hematoxylin and eosin staining, and protein expression levels were assessed using western blotting and immunohistochemical staining. In addition, apoptosis was examined using a terminal deoxynucleotidyl transferase dUTP nick-end labeling assay. The present results suggested that Dex protected against CP-induced AKI

by attenuating histological changes in the kidney, serum BUN and Scr production. Furthermore, the expression levels of 78-kDa glucose-regulated protein, C/EBP homologous protein and caspase-12, and the apoptotic rate in the kidney were decreased following Dex treatment. In addition, the expression levels of phosphorylated (p)-PI3K and p-AKT in the Dex + CP group were significantly increased. Conversely, the renoprotective effects of Dex were attenuated following the addition of Atip. In conclusion, Dex may alleviate CP-induced AKI by attenuating ERS-induced apoptosis, at least in part, via the  $\alpha_2$ AR/PI3K/AKT signaling pathway.

## Introduction

Acute kidney injury (AKI) is a frequent complication among hospitalized patients and is associated with poor clinical outcomes (1,2). Major surgery, sepsis and chemotherapeutic agent use are the leading causes of AKI (3-6). Cisplatin (CP), one of the most commonly used chemotherapeutic drugs, is used to treat a wide spectrum of human malignancies (7). However, it has been reported that 25-35% of patients experience nephrotoxicity, particularly AKI, which is a major limitation for the clinical application of CP (8,9). CP-based chemotherapy combined with surgery is widely used to treat cancer and has been demonstrated to improve postoperative survival rate (10). However, patients with cancer are often required to undergo both surgery and chemotherapy, which can exacerbate renal injury (11). A previous study reported that the incidence of AKI in patients with cancer was higher compared with in patients without cancer (12). Therefore, effective strategies to prevent AKI are essential for patients in the perioperative period.

Previous studies have focused on the development of anti-inflammatory and anti-apoptotic drugs to manage CP-induced renal injury (8,13). The endoplasmic reticulum (ER) can serve a critical role in CP cellular toxicity (13,14). The ER is the organelle responsible for synthesis and maturation of proteins, calcium storage and maintenance of cell homeostasis (15). Cellular events, such as oxidative stress, can trigger ER stress (ERS). As a protective stress response,

*Correspondence to:* Professor Huiqun Jia, Department of Anesthesiology, The Fourth Hospital of Hebei Medical University, 12 Jiankang Road, Shijiazhuang, Hebei 050011, P.R. China  
E-mail: skz688@126.com

\*Contributed equally

**Key words:** cisplatin, acute kidney injury, dexmedetomidine, endoplasmic reticulum stress, apoptosis

the homeostasis of the ER can be restored via the unfolded protein response (UPR) (16). However, in cases of severe ERS, accumulation of a large number of unfolded proteins results in the dissociation of the 78-kDa glucose-regulated protein (GRP78) from transmembrane proteins, and activation of the downstream signaling molecules C/EBP homologous protein (CHOP) and caspase-12, eventually leading to apoptosis (17). Previous studies have experimentally shown amelioration of CP-induced nephrotoxicity mediated by attenuating ERS-induced apoptosis (14,18,19). In addition, the PI3K/AKT signaling pathway has a central role in cell growth, differentiation and apoptosis (20). Using PI3K-knockout mice, it was previously revealed that a conventional dose of CP was more lethal in these knockout mice, indicating the importance of the PI3K/AKT pathway in protecting the kidneys (21).

Dexmedetomidine (Dex), a highly selective  $\alpha_2$  adrenoreceptor ( $\alpha_2$ AR) agonist, has been reported to be beneficial for the prevention of numerous types of kidney diseases, including acute stress-induced kidney injury (22), ischemia-reperfusion and sepsis-induced kidney injuries (23-25). It has also been demonstrated that Dex protects the kidney against CP-induced AKI by regulating apoptosis and the inflammatory response (26). However, the molecular mechanisms underlying the effects of Dex against CP-induced AKI have not been fully elucidated. As the pathogenesis of CP-induced AKI is mediated by ERS-induced apoptosis, Dex may be able to alleviate apoptosis by inhibiting ERS (27,28). Therefore, the present study aimed to investigate the protective effects of Dex against CP-induced AKI and assessed whether these effects were mediated by attenuation of ERS-induced apoptosis via the  $\alpha_2$ AR/PI3K/AKT pathway.

## Materials and methods

**Animals.** Animal experiments were performed in accordance with The Guiding Principles for the Care and Use of Laboratory Animals (updated 2011; National Institutes of Health) (29) and were approved by The Animal Care Committee of Hebei Medical University (Shijiazhuang, China). In total, 40 male Sprague-Dawley rats (weight, 200-220 g; age, 6 weeks) were obtained from Liaoning Chengsheng Biotechnology Co., Ltd. [certificate of conformity no. SCXK (liao) 2015-0001]. Rats were acclimated for 7 days prior to the start of the study. All rats were kept under standard conditions: Temperature ( $22\pm 2^\circ\text{C}$ ), humidity (50-60%), with a 12-h light/dark cycle, and had free access to food (standard pellet laboratory chow) and water. The rats were randomly divided into the following four groups ( $n=10/\text{group}$ ): i) Control (Con) group, rats received intraperitoneal (i.p.) injections of 0.9% saline (5 ml/kg) on days 1 and 3; ii) CP group, rats received an i.p. injection of 5 mg/kg CP (1 mg/ml, dissolved in 0.9% saline) on day 1 and an i.p. injection of 0.9% saline (10 ml/kg) on day 3; iii) Dex + CP group, rats were administered an i.p. injection of 25  $\mu\text{g}/\text{kg}$  Dex immediately after CP treatment; and iv) Dex + CP + atipamezole (Atip) group, rats received an i.p. injection of atipamezole, the  $\alpha_2$ AR antagonist, at a dose of 250  $\mu\text{g}/\text{kg}$  and then received the same treatment as the Dex + CP group. Dex and Atip were given once a day for 3 days. The doses of Dex, CP and Atip were based on previous studies (26,30). CP and Atip were purchased from Sigma-Aldrich (Merck KGaA), and

Dex was purchased from Jiangsu Hengrui Medicine Co., Ltd. The rats were weighed daily and monitored for food and water intake, and mental status. The rats were anesthetized with 2% pentobarbital solution (60 mg/kg) 96 h after treatment with CP. A total of 2 ml blood was withdrawn from the abdominal aorta, and the serum was separated by centrifugation ( $3,000 \times g$ ;  $4^\circ\text{C}$  for 20 min) and stored at  $-80^\circ\text{C}$ . Subsequently, animals were euthanized with 5% pentobarbital solution (150 mg/kg), and both kidneys were immediately excised, weighed and cut into coronal sections. In total, two pieces of the kidney were snap frozen in liquid nitrogen and stored at  $-80^\circ\text{C}$  for later use in biochemical tests and western blot analysis. A small part of the kidney was preserved in 10% neutral buffered-formalin for histological evaluations, immunohistochemistry and terminal deoxynucleotidyl transferase dUTP nick-end labeling (TUNEL) assay.

**Biochemical analysis.** Serum blood urea nitrogen (BUN) and serum creatinine (Scr) levels were assessed using commercially supplied kits (cat. nos. C010 and C074; Wuhan Servicebio Technology Co., Ltd.); samples were analyzed according to the manufacturer's instructions. The renal index (RI) was calculated as follows: Weight of both kidneys (g)/animal weight (g)  $\times 100$ .

**Histopathological analysis.** To evaluate histological changes, samples were fixed with 10% formalin buffer for 24 h at  $25^\circ\text{C}$  and then embedded in paraffin. Paraffin-embedded tissue samples were cut into 5- $\mu\text{m}$  thick sections. The tissue sections were subsequently deparaffinized in xylene ( $22\pm 2^\circ\text{C}$ ) twice for 15-20 min each and rehydrated in pure ethanol for 10 min each, followed by a descending ethanol series (95, 90, 80 and 70%) for 5 min each. Deparaffinized sections were incubated in 3% hydrogen peroxide diluted in methanol for 10 min at  $25^\circ\text{C}$  in the dark to inhibit endogenous peroxidase activity and subsequently with 3% BSA (cat. no. G5001; Wuhan Servicebio Technology Co., Ltd.) for 30 min at  $25^\circ\text{C}$  to block any non-specific binding. Tissue sections were then stained with 0.1% hematoxylin for 10 min and with 0.5% eosin for 1 min (both at  $22\pm 2^\circ\text{C}$ ). Histopathological changes were observed using a light microscope (magnification,  $\times 400$ ; Leica Microsystems GmbH). Assessment of the tubular damage score was performed in 10 fields in five sections per group using the following index of renal tubular necrosis: Score of 0 (absence of damage); score of 1 ( $<25\%$  damage); score of 2 (25-50% damage); score of 3 (50-75% damage); and score of 4 ( $>75\%$  damage). Tubular necrosis was characterized by loss of the proximal tubular brush border, blebbing of apical membranes, epithelial detachment from the basement membrane or intraluminal hyaline cast formation.

**TUNEL staining analysis.** The TUNEL assay (cat. no. 116848179; Roche Diagnostics GmbH) was conducted according to the manufacturer's instructions. Tissues were fixed and prepared in the same manner as for histopathology and subsequently, deparaffinized tissue sections were incubated with 3% hydrogen peroxide in methanol for 10 min at  $15-25^\circ\text{C}$  in the dark, washed three times with PBS and incubated with 0.1% Triton X-100 in freshly prepared 0.01%

sodium citrate for 8 min at 25°C. Tissue sections were then incubated with proteinase K working solution (cat. no. G1205; Wuhan Servicebio Technology Co., Ltd.) for 25 min at 37°C and washed three times with PBS (pH 7.4) in a Rocker device for 5 min each. Reagent 1 (TdT) and reagent 2 (dUTP; both from the TUNEL assay kit) were mixed at a ratio of 1:9 and the mixture was incubated with the tissue sections at 37°C for 2 h. The sections were washed three times with PBS (pH 7.4) and then cell nuclei were counterstained with 2 µg/ml DAPI solution (cat. no. G1012; Wuhan Servicebio Technology Co., Ltd.) at room temperature for 10 min in the dark and mounted with 50 µl anti-fade mounting medium (cat. no. G1401; Wuhan Servicebio Technology Co., Ltd.). TUNEL-positive cells were observed in five randomly-selected fields using a fluorescence microscope (magnification, x400); the nucleus is blue and positive apoptotic cells are green. The number of positive cells per high-power field was calculated and analyzed in a blinded manner using Image-Pro Plus 6.0 software (Media Cybernetics, Inc.).

**Immunohistochemical analysis.** For immunohistochemical analysis, kidney tissues were fixed with 10% formaldehyde solution for 24 h at 15–25°C. Subsequently, tissues were embedded in paraffin and cut into 5-µm sections. Deparaffinization of the sections was followed by heating for 10 min at 95°C in citrate buffer solution (0.01 M; pH 6.0). The slides were then washed with TBS (0.01 M; pH 7.4) and incubated with 10% goat serum (Wuhan Servicebio Technology Co., Ltd.) for 60 min at 37°C and with primary antibodies at 4°C overnight. The primary antibodies used were anti-GRP78 (1:200; cat. no. ab21685; Abcam) and anti-caspase-12 (1:100; cat. no. ab62484; Abcam). After three washes with PBS, the sections were incubated with a horseradish peroxidase (HRP)-conjugated goat secondary antibody (1:200; cat. no. G1213; Wuhan Servicebio Technology Co., Ltd.) for 30 min at 37°C. To count stained nuclei, 0.1% hematoxylin staining for 10 min at 22±2°C was performed. Analysis was performed using Leica QWin V3 image analysis software (Leica Microsystems GmbH). Brown areas of staining were considered as positive. The intensity of the staining was graded as follows: 0 (no color); 1 (light yellow); 2 (light brown); and 3 (brown). The percentage of positively stained areas was graded as follows: 0 (<5%); 1 (5–25%); 2 (25–50%); 3 (51–75%); and 4 (>75%). In total, ten high-power fields (magnification, x400) per section were randomly selected using light microscopy, and two sections per kidney per group were examined in each experiment.

**Western blotting.** Renal tissues were lysed with RIPA buffer (cat. no. G2002; Wuhan Servicebio Technology Co., Ltd), supplemented with 1 mM PMSF and homogenized. The homogenate was centrifuged at 4,000 × g for 20 min at 4°C, and the supernatant was collected and measured for protein concentration using a bicinchoninic acid protein assay kit (cat. no. G2026; Wuhan Servicebio Technology Co., Ltd.). Equal amounts of protein (40 µg) from each sample were separated by 10–12% SDS-PAGE and electrotransferred onto a PVDF membrane and blocked with 5% skimmed milk at room temperature for 2 h on a rotating shaker. Membranes were subsequently washed with TBS-0.1% Tween (TBST). The primary antibodies used were as follows: GRP78 (1:1,000;

rabbit; cat. no. ab21685; Abcam), CHOP (1:1,000; rabbit; cat. no. 2895; Cell Signaling Technology, Inc.), caspase-12 (1:600; rabbit; cat. no. ab62484; Abcam), AKT (1:1,000; rabbit; cat. no. AF6261; Affinity Biosciences), phosphorylated (p)-AKT (1:1,000; rabbit; cat. no. AF0832; Affinity Biosciences), PI3K (1:1,000; rabbit; cat. no. AF6241; Affinity Biosciences), p-PI3K (1:1,000; rabbit; cat. no. AF3241; Affinity Biosciences) and β-actin (1:3,000; mouse; cat. no. GB12001; Wuhan Servicebio Technology Co., Ltd.). Membranes were incubated with antibodies overnight at 4°C. After washing three times in TBST, the membranes were incubated with HRP-conjugated secondary antibodies (1:3,000; cat. nos. GB23302 and GB23303; Wuhan Servicebio Technology Co., Ltd.) for 2 h at room temperature. Bands were detected using standard ECL (EMD Millipore). The band intensity was measured using ImageJ version 8.0 software (National Institutes of Health).

**Statistical analysis.** The statistical analyses were performed, and the graphs were created using GraphPad Prism (version 7.0; GraphPad Software, Inc.). Data are presented as the mean ± SEM of between 3–10 experimental repeats. Variables were checked for normal distribution using the Shapiro-Wilk test. Data were analyzed using one-way ANOVA followed by Tukey's multiple comparisons testing as appropriate. The histopathological and immunohistochemical data were compared using Kruskal-Wallis test followed by Dunn's multiple comparisons test. P<0.05 was considered to indicate a statistically significant difference.

## Results

**Dex treatment rescues the change in body weight and RI.** A previous study suggested that CP could reduce body weight in rats (31). In the present study, animal models of CP-induced AKI were established by i.p. injection of 5 mg/kg CP. It was revealed that CP-treated animals lost a significant amount of weight and exhibited increased RI compared with the Con group (Fig. 1A and B; P<0.001). However, administration of Dex in combination with CP significantly rescued the alteration in body weight and RI compared with the CP group (P<0.05). Moreover, treatment with Atip in combination with Dex resulted in a similar outcome to the CP group (Fig. 1A and B; P<0.05).

**Dex treatment ameliorates CP-induced nephrotoxicity markers.** Clinical markers for renal tissue injury, including the levels of serum BUN and Scr, were investigated to evaluate CP-induced nephrotoxicity. It has previously been reported that a single dose of CP (3–8 mg/kg) can cause acute nephrotoxicity and induce changes to kidney structure and function in rats (32). In the present study, animal models of CP-induced AKI were established by i.p. injection of 5 mg/kg CP. It was demonstrated that rats in the CP-treated group developed renal dysfunction and exhibited significantly increased Scr and BUN levels compared with the Con group (Fig. 1C and D; P<0.001). However, Scr and BUN expression levels in the Dex + CP group were significantly lower compared with the CP group (P<0.01). Furthermore, the renoprotective effects of Dex were reversed by treatment with the α2AR antagonist Atip (Fig. 1C and D; P<0.01).

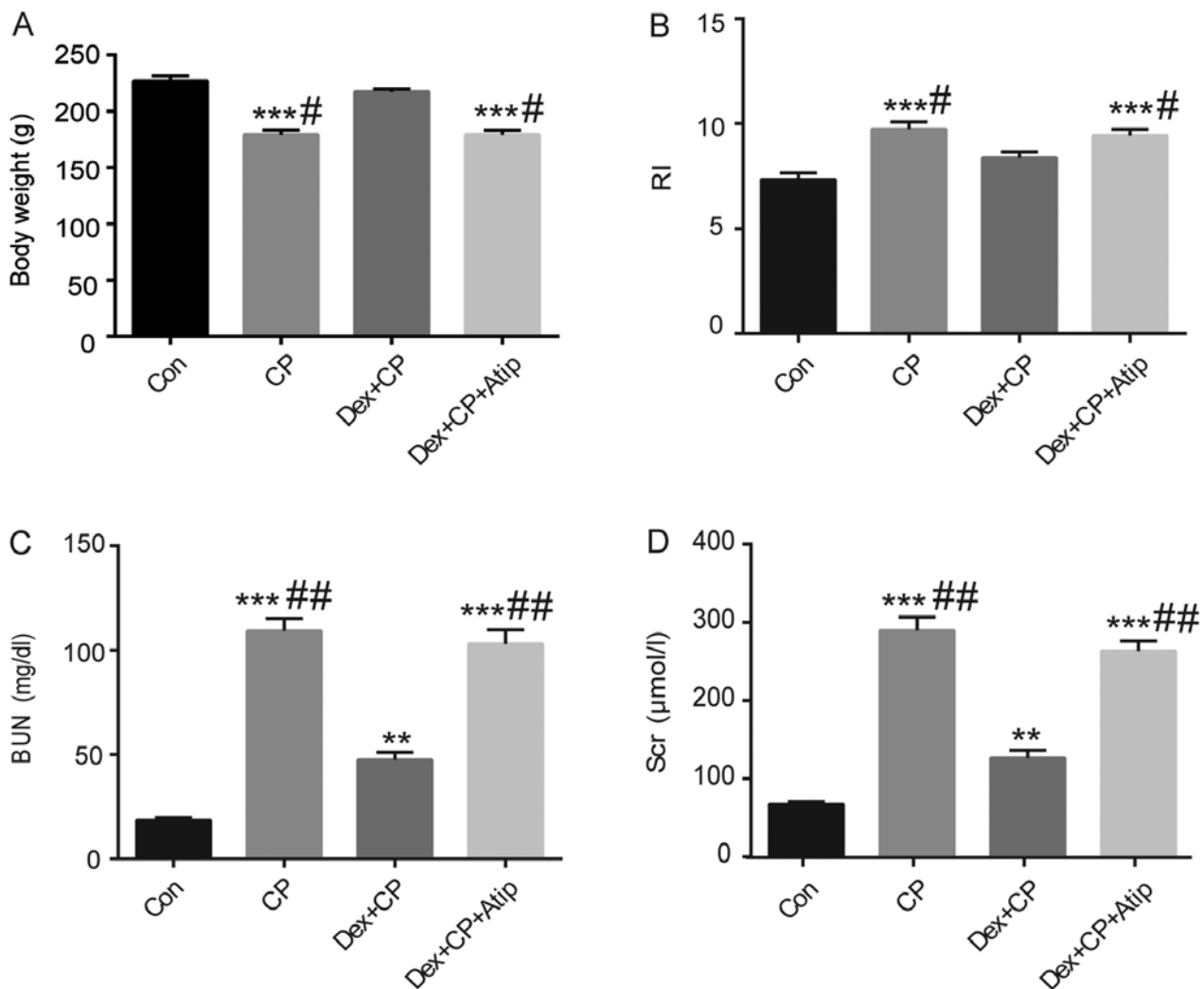


Figure 1. Effect of Dex on renal function and body weight. (A) Body weight, (B) RI, (C) BUN and (D) Scr. Data are presented as the mean  $\pm$  SEM (n=10). \*\*P<0.01, \*\*\*P<0.001 vs. Con; #P<0.05, ##P<0.01 vs. Dex + CP. Atip, atipamezole; BUN, blood urea nitrogen; Con, control; CP, cisplatin; Dex, dexmedetomidine; Scr, serum creatinine; RI, renal index.

*Dex treatment ameliorates CP-induced kidney tubular damage.* H&E staining was performed to investigate the renoprotective effects of Dex following CP administration. The histological examination results suggested that the kidneys from the Con and Dex + CP groups exhibited normal tubular morphology, whereas the kidneys from the CP group showed severe tubular damage and widespread tubular necrosis, with dilatation and tubular atrophy (Fig. 2A). In addition, the extent of histological damage in the CP group was significantly higher compared with the Con group (P<0.001; Fig. 2B). However, the extent of tubular damage was significantly reduced in the Dex + CP group compared with the CP group (P<0.05; Fig. 2A and B). Furthermore, the  $\alpha$ 2 receptor blocker Atip abolished the effects of Dex (P<0.05; Fig. 2A and B).

*Dex treatment ameliorates CP-induced apoptosis of tubular epithelial cells.* Apoptotic cell death is the major pathological process which renal tissue undergoes as a result of CP toxicity (32). To investigate whether Dex protected renal tubular epithelial cells against apoptosis induced by CP, tubular cell apoptosis was detected in the present CP-induced AKI model using TUNEL assay. It was revealed that apop-

totic cell death, characterized by TUNEL-positive cells, was significantly increased in the CP group compared with the Con group (P<0.001; Fig. 3A and B). Dex administration significantly reduced the number of TUNEL-positive cells in the kidneys after CP treatment (P<0.05), indicating reduced apoptosis in the Dex + CP group. In addition, Atip reversed the renoprotective effects of Dex (P<0.05; Fig. 3B), indicating that the  $\alpha$ 2AR blocker atipamezole abolished the protective effects of Dex on apoptotic cell death.

*Dex treatment ameliorates the expression of GRP78, CHOP and caspase-12.* A previous study has also demonstrated that ERS-mediated apoptotic pathways are implicated in CP-induced AKI (6). Therefore, to investigate the mechanisms underlying the renoprotective effects of Dex, the expression levels of GRP78, CHOP and caspase-12, which are major proteins involved in ERS-mediated apoptosis (33), were examined. The present results suggested that the protein expression levels of GRP78, CHOP and caspase-12 were significantly increased in the CP group compared with the Con group (P<0.01; Fig. 4A-D). However, the expression levels of these proteins were significantly reduced in the Dex-treated group (P<0.05

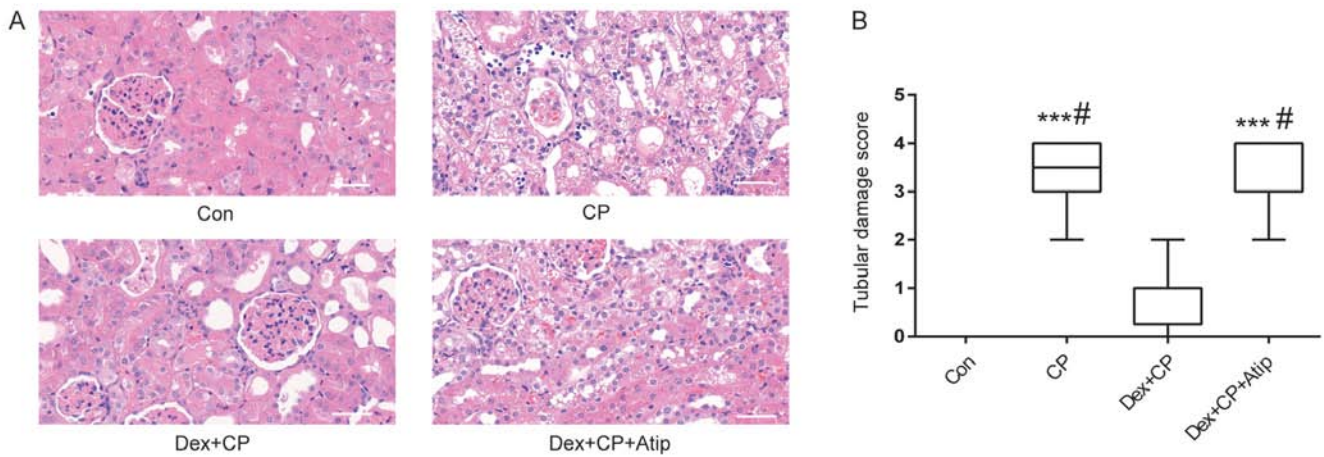


Figure 2. Dex attenuates CP-induced kidney tubular damage. (A) Histological examination of sections stained with hematoxylin and eosin staining (magnification, x400; scale bar, 50  $\mu$ m). (B) Tubular damage scores. Data are presented as the mean  $\pm$  SEM (n=10). \*\*\*P<0.001 vs. Con; #P<0.05 vs. Dex + CP. Atip, atipamezole; Con, control; CP, cisplatin; Dex, dexmedetomidine.

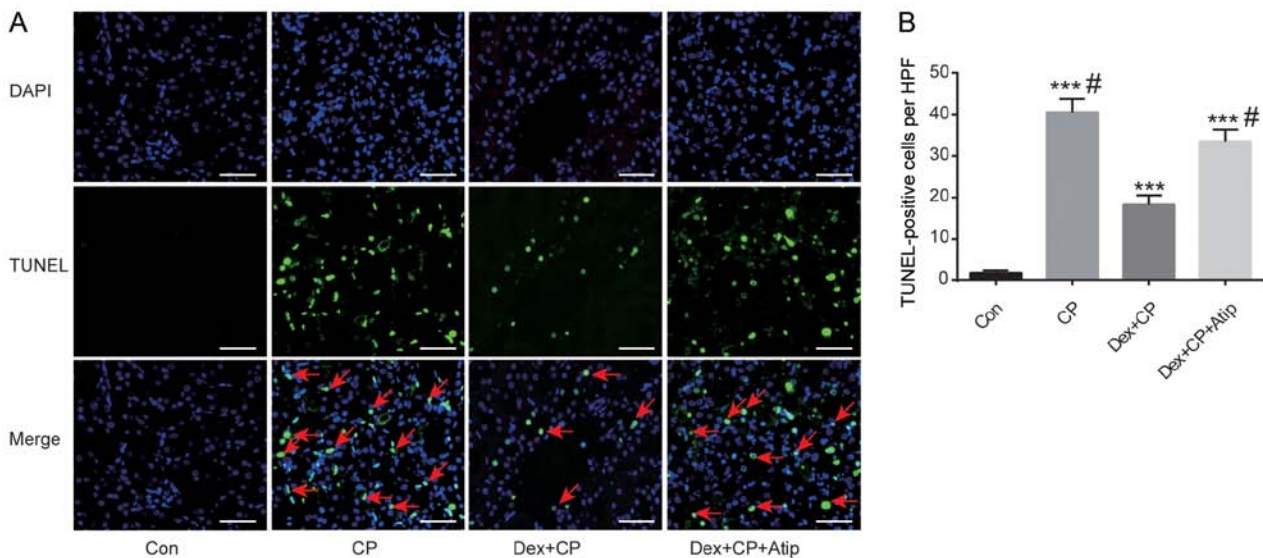


Figure 3. Dex protects against proximal tubular cell apoptosis induced by CP. (A) TUNEL staining assay (magnification, x400; scale bar, 50  $\mu$ m). Green, TUNEL; blue, DAPI; red arrows, TUNEL-positive cells. (B) Quantification of TUNEL-positive cells. Data are presented as the mean  $\pm$  SEM (n=10). \*\*\*P<0.001 vs. Con; #P<0.05 vs. Dex + CP. Atip, atipamezole; Con, control; CP, cisplatin; Dex, dexmedetomidine; HPF, high-power field; TUNEL, terminal deoxynucleotidyl transferase dUTP nick-end labelling.

and P<0.01). The present study also investigated the expression levels of GRP78 and caspase-12 using immunohistochemical staining (Fig. 4H). The immunohistochemistry results of GRP78 and caspase-12 protein expression were consistent with the western blotting results, where CP treatment increased the expression levels of GRP78 and caspase-12 compared with the Con group (P<0.01 and P<0.05; Fig. 4I and J). Moreover, Dex treatment significantly reduced CP-induced GRP78 and caspase-12 expression, whereas Atip reversed the renoprotective effects of Dex (P<0.01; Fig. 4I and J).

**Dex treatment regulates the PI3K/AKT signaling pathway.** Activation of the PI3K/AKT pathway serves a key role in cytoprotective signaling and has been demonstrated to exert protective effects against CP-induced renal toxicity (34). A previous study reported that Dex activates the cell survival PI3K/AKT signaling pathway via  $\alpha$ 2AR in order to provide

renoprotection (35). To investigate whether Dex activated the PI3K/AKT signaling pathway, the present study measured the expression levels of p-PI3K and p-AKT. The results revealed that the protein expression levels of p-PI3K and p-AKT were significantly decreased in the CP group compared with the Dex + CP group (P<0.05 and P<0.01; Fig. 4E-G), indicating that Dex activated the PI3K/AKT signaling pathway. Treatment with Atip in combination with Dex resulted in a similar outcome to CP; Dex + CP + Atip decreased the protein expression levels of p-PI3K and p-AKT compared with the CP + Dex group (P<0.05; Fig. 4F and G).

**Discussion**

CP is known to induce AKI as a result of renal tubular epithelial cell injury. ERS-induced apoptosis of tubular epithelium cells serves a pivotal role in the pathogenesis of CP-induced

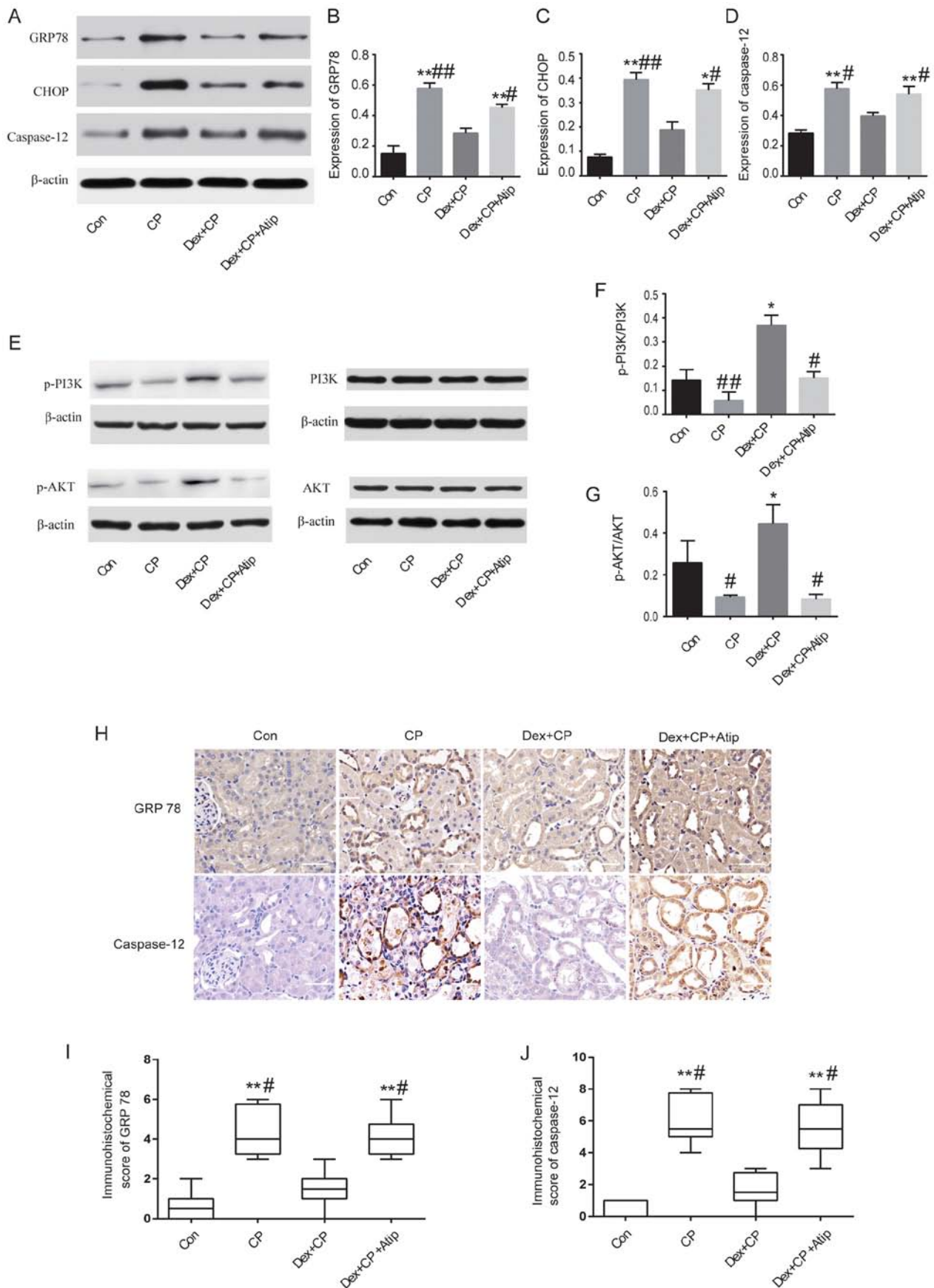


Figure 4. Western blot analysis and immunohistochemical staining of proteins in the kidney. (A) Western blot analysis, and semi-quantification of protein expression levels of (B) GRP78, (C) CHOP and (D) caspase-12. (E) Western blot analysis, and semi-quantification of protein expression levels of (F) p-PI3K/PI3K (G) and p-AKT/AKT relative to  $\beta$ -actin control. (H) Expression levels of GRP78 and caspase-12 detected in damaged tubules by immunohistochemistry (magnification,  $\times 400$ ; scale bar,  $50 \mu\text{m}$ ). (I) Semi-quantification of GRP78 in kidney sections. (J) Semi-quantification of caspase-12 in kidney sections. Data are presented as the mean  $\pm$  SEM ( $n=3$ ). \* $P<0.05$ , \*\* $P<0.01$  vs. Con; # $P<0.05$ , ## $P<0.01$  vs. Dex + CP. Atip, atipamezole; CHOP, C/EBP homologous protein; Con, control; CP, cisplatin; Dex, dexmedetomidine; GRP78, 78-kDa glucose-regulated protein; p-, phosphorylated.

nephrotoxicity (9,36). Therefore, the present study investigated whether Dex exerted a renoprotective effect on CP-induced AKI in a rat model by inhibiting ERS-mediated apoptosis via the  $\alpha$ 2AR/PI3K/AKT pathway. The present results suggested that Dex facilitated a significant reduction in RI, body weight, and Scr and BUN levels, indicating a significant renoprotective effect, which was further demonstrated by H&E staining and apoptosis analysis. In addition, Dex reduced the expression levels of ERS-dependent proteins and increased the expression levels of p-PI3K and p-AKT. Furthermore, the  $\alpha$ 2 receptor blocker Atip abolished the effects of Dex. Therefore, the protective mechanism underlying Dex may be related to ERS-mediated apoptosis via the  $\alpha$ 2AR/PI3K/AKT signaling pathway. The present results provided a novel insight into the biological benefits of Dex as a potential renoprotective agent.

As biomarkers of renal function, BUN and Scr are often used to reflect the degree of renal injury (37). In the present study, BUN and Scr levels in the CP group were significantly increased, and body weight and RI were significantly changed, compared with in the Con group. Furthermore, the results of histopathological examination and TUNEL assay revealed that CP aggravated kidney damage compared with the Con group. The present results were consistent with those from previous studies (38). In the present study, Dex administration significantly inhibited the production of serum BUN and Scr and reversed the alterations in body weight and RI. Furthermore, Atip abolished the effects of Dex. The present study identified the beneficial effects of Dex on prevention of renal tubular damage and dysfunction. However, the mechanism underlying this protective effect requires further investigation.

The ER is an intracellular organelle that serves an important role in protein homeostasis (14). The ER can restore homeostasis via the UPR. When the UPR fails to protect cells, ERS becomes one of the main pathogenic factors that induces the apoptotic pathway and results in an accumulation of misfolded proteins (6). As a major response to ERS, GRP78 is released from transmembrane proteins and activates protein kinase RNA-like ER kinase (PERK), inositol requiring enzyme 1 (IRE1) and activating transcription factor 6 (ATF6), which induce the pro-apoptotic transcription factor CHOP, eventually leading to apoptosis (39). Caspase-12, a marker of apoptosis, is localized on the ER and is specifically activated via ERS, and not via membrane or mitochondrial signals. It has been reported that ERS-mediated apoptosis is important in CP-induced nephrotoxicity, suggesting that ER is a target of CP, and that GRP78, caspase-12 and CHOP are important molecules (9,40,41).

To investigate the mechanisms underlying the protective effects of Dex against CP-induced tubular cell apoptosis, the present study examined the protein expression levels of GRP78, CHOP and caspase-12. It was revealed that GRP78, CHOP and caspase-12 protein expression was increased following treatment with CP, whereas Dex treatment significantly inhibited the expression of these proteins. Therefore, the present results suggested that Dex could suppress CP-induced ERS. Previous studies have shown that the neuroprotective and cardioprotective effects of Dex are mediated by inhibiting ERS-dependent apoptosis (27,42). Furthermore, Liang *et al* (26) reported that Dex exerted an anti-inflammatory effect via inhibition of the NF- $\kappa$ B signaling pathway and had a role in the inhibition of

apoptosis via p53-mediated Bax induction during CP-induced AKI. The present study also examined whether the  $\alpha$ 2AR served a role in the protective effect of Dex. The present results suggested that the  $\alpha$ 2AR antagonist Atip reversed the renoprotective effects of Dex, indicating that Dex acted in an  $\alpha$ 2AR-dependent manner. Gu *et al* (35) revealed that Dex exerted a renoprotective effect against ischemia-reperfusion injury via the  $\alpha$ 2AR-dependent pathway. Therefore, the present results indicated that the potential mechanism underlying the effects of Dex on the prevention of CP-induced AKI may be associated with the suppression of ERS-mediated apoptosis via activation of  $\alpha$ 2AR.

The PI3K/AKT signaling pathway has a major role in promoting cell survival by inhibiting the caspase-controlled intrinsic apoptotic pathway (43). A previous study has shown that ERS-induced apoptosis is closely associated with the PI3K/AKT signaling pathway (44). In addition, CP aggravates renal injury by inhibiting the PI3K/AKT signaling pathway in rat kidneys (45), and a conventional dose of CP is more lethal in PI3K-knockout mice (21). The present study identified a significant increase in the expression levels of p-AKT following treatment with Dex in CP-induced AKI. However, treatment with CP + Dex + Atip had a similar effect to CP alone; the expression levels of p-PI3K and p-AKT were significantly decreased in the CP + Dex + Atip group, indicating that the effects of Dex were partially blocked by the  $\alpha$ 2AR antagonist. Furthermore, a previous study reported that AKT signaling is critical for recovery from renal ischemia-reperfusion injury, and that Dex activates AKT via  $\alpha$ 2AR-dependent and -independent PI3K coupling (38). Similarly, Dex exerts neuroprotective (46), cardioprotective (28) and lung-protective effects (30,47) via activation of the PI3K/AKT signaling pathway. Therefore, the protective effects of Dex against CP-induced AKI may involve AKT signaling.

There were some limitations to the present study. The present results suggested that Dex alleviated CP-induced AKI by attenuating ERS-induced apoptosis, at least in part, via the  $\alpha$ 2AR/PI3K/AKT pathway. Since this study used an *in vivo* model, the renoprotective effect of Dex may be associated with other unidentified mechanisms, and whether Dex is able to directly protect renal tubular epithelial cells remains unclear. Furthermore, ERS is a complex process involving three transmembrane proteins, PERK, ATF6 and IRE1, which are bound to GRP78 (48). The present study did not detect changes in these transmembrane proteins; therefore, it is not clear which membrane protein is involved in the renoprotective effects of Dex. In addition, the activated status of caspase-12 is based on the cleavage of procaspase-12 (30), and the present study did not detect changes in the cleavage status of procaspase-12, which may not accurately express changes in ERS. Furthermore, the sample sizes were relatively small in the present study. Therefore, the present results may have false-positive and false-negative errors. The mechanism underlying the effects of Dex is complex and further in-depth research is required to fully understand the effects of Dex.

In conclusion, the present results suggested that Dex may protect against CP-induced AKI, and the underlying mechanism may be associated with the suppression of ERS-mediated apoptosis via the  $\alpha$ 2AR/PI3K/AKT signaling pathway. These results provided an insight into

the novel biological benefits of Dex as a renoprotective agent for patients with cancer. However, the pathological process of CP-induced AKI involves a variety of complex mechanisms, and whilst Dex has a protective effect, it requires further study to be used as a therapeutic tool in clinical settings.

### Acknowledgements

Not applicable.

### Funding

No funding was received.

### Availability of data and materials

All data generated or analyzed during the present study are included in this published manuscript.

### Authors' contributions

HQJ and KSZ designed the experiments. YJC, KSZ and XFW performed the experiments. KSZ, JMS, FFY and CL analyzed the data and prepared the images. KSZ and YJC drafted the manuscript. All authors reviewed the manuscript.

### Ethics approval and consent to participate

The present study was approved by The Animal Care Committee of Hebei Medical University.

### Patient consent for publication

Not applicable.

### Competing interests

The authors declare that they have no competing interests.

### References

- Al-Jaghbeer M, Dealmeida D, Bilderback A, Ambrosino R and Kellum JA: Clinical decision support for in-hospital AKI. *J Am Soc Nephrol* 29: 654-660, 2018.
- Zarbock A, Koyner JL, Hoste EAJ and Kellum JA: Update on perioperative acute kidney injury. *Anesth Analg* 127: 1236-1245, 2018.
- Chertow GM, Burdick E, Honour M, Bonventre JV and Bates DW: Acute kidney injury, mortality, length of stay, and costs in hospitalized patients. *J Am Soc Nephrol* 16: 3365-3370, 2005.
- Gameiro J, Fonseca JA, Neves M, Jorge S and Lopes JA: Acute kidney injury in major abdominal surgery: Incidence, risk factors, pathogenesis and outcomes. *Ann Intensive Care* 8: 22, 2018.
- Jin J, Wang Y, Shen Q, Gong J, Zhao L and He Q: Acute kidney injury in cancer patients: A nationwide survey in China. *Sci Rep* 9: 3540, 2019.
- Izzedine H and Perazella MA: Anticancer drug-induced acute kidney injury. *Kidney Int Rep* 2: 504-514, 2017.
- Dilruba S and Kalayda GV: Platinum-based drugs: Past, present and future. *Cancer Chemother Pharmacol* 77: 1103-1124, 2016.
- Pabla N and Dong Z: Cisplatin nephrotoxicity: Mechanisms and renoprotective strategies. *Kidney Int* 73: 994-1007, 2008.
- Manohar S and Leung N: Cisplatin nephrotoxicity: A review of the literature. *J Nephrol* 31: 15-25, 2018.
- Miao ZF, Liu XY, Wang ZN, Zhao TT, Xu YY, Song YX, Huang JY, Xu H and Xu HM: Effect of neoadjuvant chemotherapy in patients with gastric cancer: A PRISMA-compliant systematic review and meta-analysis. *BMC Cancer* 18: 118, 2018.
- Lee EH, Kim HR, Baek SH, Kim KM, Chin JH, Choi DK, Kim WJ and Choi IC: Risk factors of postoperative acute kidney injury in patients undergoing esophageal cancer surgery. *J Cardiothorac Vasc Anesth* 28: 936-942, 2014.
- Salahudeen AK, Doshi SM, Pawar T, Nowshad G, Lahoti A and Shah P: Incidence rate, clinical correlates, and outcomes of AKI in patients admitted to a comprehensive cancer center. *Clin J Am Soc Nephrol* 8: 347-354, 2013.
- Oh GS, Kim HJ, Shen A, Lee SB, Khadka D, Pandit A and So HS: Cisplatin-induced kidney dysfunction and perspectives on improving treatment strategies. *Electrolyte Blood Press* 12: 55-65, 2014.
- Yan M, Shu S, Guo C, Tang C and Dong Z: Endoplasmic reticulum stress in ischemic and nephrotoxic acute kidney injury. *Ann Med* 50: 381-390, 2018.
- Volarevic V, Djokovic B, Jankovic MG, Harrell CR, Fellabaum C, Djonov V and Arsenijevic N: Molecular mechanisms of cisplatin-induced nephrotoxicity: A balance on the knife edge between renoprotection and tumor toxicity. *J Biomed Sci* 26: 25, 2019.
- Bravo R, Parra V, Gatica D, Rodriguez AE, Torrealba N, Paredes F, Wang ZV, Zorzano A, Hill JA, Jaimovich E, *et al*: Endoplasmic reticulum and the unfolded protein response: Dynamics and metabolic integration. *Int Rev Cell Mol Biol* 301: 215-290, 2013.
- García de la Cadena S and Massieu L: Caspases and their role in inflammation and ischemic neuronal death. *Focus on caspase-12*. *Apoptosis* 21: 763-777, 2016.
- Chen B, Liu G, Zou P, Li X, Hao Q, Jiang B, Yang X and Hu Z: Epigallocatechin-3-gallate protects against cisplatin-induced nephrotoxicity by inhibiting endoplasmic reticulum stress-induced apoptosis. *Exp Biol Med (Maywood)* 240: 1513-1519, 2015.
- Gao Z, Liu G, Hu Z, Li X, Yang X, Jiang B and Li X: Grape seed proanthocyanidin extract protects from cisplatin-induced nephrotoxicity by inhibiting endoplasmic reticulum stress-induced apoptosis. *Mol Med Report* 9: 801-807, 2014.
- Gong X, Shao L, Fu YM and Zou Y: Effects of olmesartan on endothelial progenitor cell mobilization and function in carotid atherosclerosis. *Med Sci Monit* 21: 1189-1193, 2015.
- Kuwana H, Terada Y, Kobayashi T, Okado T, Penninger JM, Irie-Sasaki J, Sasaki T and Sasaki S: The phosphoinositide-3 kinase gamma-Akt pathway mediates renal tubular injury in cisplatin nephrotoxicity. *Kidney Int* 73: 430-445, 2008.
- Chen Y, Feng X, Hu X, Sha J, Li B, Zhang H and Fan H: Dexmedetomidine ameliorates acute stress-induced kidney injury by attenuating oxidative stress and apoptosis through inhibition of the ROS/JNK signaling pathway. *Oxid Med Cell Longev* 2018: 4035310, 2018.
- Chen Y, Luan L, Wang C, Song M, Zhao Y, Yao Y, Yang H, Ma B and Fan H: Dexmedetomidine protects against lipopolysaccharide-induced early acute kidney injury by inhibiting the iNOS/NO signaling pathway in rats. *Nitric Oxide* 85: 1-9, 2019.
- Si Y, Bao H, Han L, Chen L, Zeng L, Jing L, Xing Y and Geng Y: Dexmedetomidine attenuation of renal ischaemia-reperfusion injury requires sirtuin 3 activation. *Br J Anaesth* 121: 1260-1271, 2018.
- Qiu R, Yao W, Ji H, Yuan D, Gao X, Sha W, Wang F, Huang P and Hei Z: Dexmedetomidine restores septic renal function via promoting inflammation resolution in a rat sepsis model. *Life Sci* 204: 1-8, 2018.
- Liang H, Liu HZ, Wang HB, Zhong JY, Yang CX and Zhang B: Dexmedetomidine protects against cisplatin-induced acute kidney injury in mice through regulating apoptosis and inflammation. *Inflamm Res* 66: 399-411, 2017.
- Liu C, Fu Q, Mu R, Wang F, Zhou C, Zhang L, Yu B, Zhang Y, Fang T and Tian F: Dexmedetomidine alleviates cerebral ischemia-reperfusion injury by inhibiting endoplasmic reticulum stress dependent apoptosis through the PERK-CHOP-Caspase-11 pathway. *Brain Res* 1701: 246-254, 2018.
- Cheng XY, Gu XY, Gao Q, Zong QF, Li XH and Zhang Y: Effects of dexmedetomidine postconditioning on myocardial ischemia and the role of the PI3K/Akt-dependent signaling pathway in reperfusion injury. *Mol Med Rep* 14: 797-803, 2016.

29. National Research Council: Guide for the care and use of laboratory animals: Eighth edition. Washington, DC, The National Academies Press, 2011.
30. Zhang W, Zhang JQ, Meng FM and Xue FS: Dexmedetomidine protects against lung ischemia-reperfusion injury by the PI3K/Akt/HIF-1 $\alpha$  signaling pathway. *J Anesth* 30: 826-833, 2016.
31. Alhoshani AR, Hafez MM, Husain S, Al-Sheikh AM, Alotaibi MR, Al Rejaie SS, Alshammari MA, Almutairi MM and Al-Shabanah OA: Protective effect of rutin supplementation against cisplatin-induced Nephrotoxicity in rats. *BMC Nephrol* 18: 194, 2017.
32. Perše M and Večerić-Haler Ž: Cisplatin-induced rodent model of kidney injury: Characteristics and challenges. *Biomed Res Int* 2018: 1462802, 2018.
33. Schröder M and Kaufman RJ: The mammalian unfolded protein response. *Annu Rev Biochem* 74: 739-789, 2005.
34. Potočnjak I and Domitrović R: Carvacrol attenuates acute kidney injury induced by cisplatin through suppression of ERK and PI3K/Akt activation. *Food Chem Toxicol* 98: 251-261, 2016.
35. Gu J, Sun P, Zhao H, Watts HR, Sanders RD, Terrando N, Xia P, Maze M and Ma D: Dexmedetomidine provides renoprotection against ischemia-reperfusion injury in mice. *Crit Care* 15: R153, 2011.
36. Mahgoub E, Kumaraswamy SM, Kader KH, Venkataraman B, Ojha S, Adeghate E and Rajesh M: Genipin attenuates cisplatin-induced nephrotoxicity by counteracting oxidative stress, inflammation, and apoptosis. *Biomed Pharmacother* 93: 1083-1097, 2017.
37. Zhang L, Gu Y, Li H, Cao H, Liu B, Zhang H and Shao F: Daphnetin protects against cisplatin-induced nephrotoxicity by inhibiting inflammatory and oxidative response. *Int Immunopharmacol* 65: 402-407, 2018.
38. Zhang W, Hou J, Yan X, Leng J, Li R, Zhang J, Xing J, Chen C, Wang Z and Li W: Platycodon grandiflorum saponins ameliorate cisplatin-induced acute nephrotoxicity through the NF- $\kappa$ B-mediated inflammation and PI3K/Akt/apoptosis signaling pathways. *Nutrients* 10: pii: E1328, 2018.
39. Lin JH, Li H, Yasumura D, Cohen HR, Zhang C, Panning B, Shokat KM, Lavail MM and Walter P: IRE1 signaling affects cell fate during the unfolded protein response. *Science* 318: 944-949, 2007.
40. Soni KK, Kim HK, Choi BR, Karna KK, You JH, Cha JS, Shin YS, Lee SW, Kim CY and Park JK: Dose-dependent effects of cisplatin on the severity of testicular injury in Sprague Dawley rats: Reactive oxygen species and endoplasmic reticulum stress. *Drug Des Devel Ther* 10: 3959-3968, 2016.
41. Singh MP, Chauhan AK and Kang SC: Morin hydrate ameliorates cisplatin-induced ER stress, inflammation and autophagy in HEK-293 cells and mice kidney via PARP-1 regulation. *Int Immunopharmacol* 56: 156-167, 2018.
42. Liu XR, Li T, Cao L, Yu YY, Chen LL, Fan XH, Yang BB and Tan XQ: Dexmedetomidine attenuates H<sub>2</sub>O<sub>2</sub>-induced neonatal rat cardiomyocytes apoptosis through mitochondria- and ER-mediated oxidative stress pathways. *Mol Med Report* 17: 7258-7264, 2018.
43. Fruman DA, Meyers RE and Cantley LC: Phosphoinositide kinases. *Annu Rev Biochem* 67: 481-507, 1998.
44. Zhou MF, Feng ZP, Ou YC, Peng JJ, Li K, Gong HD, Qiu BH, Liu YW, Wang YJ and Qi ST: Endoplasmic reticulum stress induces apoptosis of arginine vasopressin neurons in central diabetes insipidus via PI3K/Akt pathway. *CNS Neurosci Ther* 25: 562-574, 2019.
45. Kong D, Zhuo L, Gao C, Shi S, Wang N, Huang Z, Li W and Hao L: Erythropoietin protects against cisplatin-induced nephrotoxicity by attenuating endoplasmic reticulum stress-induced apoptosis. *J Nephrol* 26: 219-227, 2013.
46. Shen M, Wang S, Wen X, Han XR, Wang YJ, Zhou XM, Zhang MH, Wu DM, Lu J and Zheng YL: Dexmedetomidine exerts neuroprotective effect via the activation of the PI3K/Akt/mTOR signaling pathway in rats with traumatic brain injury. *Biomed Pharmacother* 95: 885-893, 2017.
47. Oyadomari S and Mori M: Roles of CHOP/GADD153 in endoplasmic reticulum stress. *Cell Death Differ* 11: 381-389, 2004.
48. Wu CT, Sheu ML, Tsai KS, Weng TI, Chiang CK and Liu SH: The role of endoplasmic reticulum stress-related unfolded protein response in the radiocontrast medium-induced renal tubular cell injury. *Toxicol Sci* 114: 295-301, 2010.



This work is licensed under a Creative Commons Attribution-NonCommercial-NoDerivatives 4.0 International (CC BY-NC-ND 4.0) License.